The martensitic phase transition in Ni–Al: experimental observation of excess entropy and heterogeneous spontaneous strain

2008 J. Phys.: Condens. Matter 20 055220

(http://iopscience.iop.org/0953-8984/20/5/055220)

J. Phys.: Condens. Matter **20** (2008) 055220 (7pp) doi:10.1088/0953-8984/20/5/055220

The martensitic phase transition in Ni–Al: experimental observation of excess entropy and heterogeneous spontaneous strain

H Zhang[1], E K H Salje[1], D Schryvers[2] and B Bartova[2]

[1] Department of Earth Sciences, University of Cambridge, Downing Street, Cambridge CB2 3EQ, UK
[2] EMAT, University of Antwerp, Groenenborgerlaan 171, B-2020 Antwerp, Belgium

Received 5 September 2007, in final form 18 December 2007
Published 18 January 2008
Online at stacks.iop.org/JPhysCM/20/055220

Abstract

Experimental studies of the martensitic phase transition of $Ni_{63.5}Al_{36.5}$ by means of differential scanning calorimetry and x-ray diffraction show a coexistence interval of 30 K for the austenite and martensitic phase. Within a smaller interval of 10 K near the upper limit of the stability of the martensitic phase no strain broadening of x-ray diffraction lines was observed for either phase. With decreasing temperature, diffraction profiles broaden, with a maximum reached when the sample is fully transformed into the martensitic phase. This observation is analyzed in terms of heterogeneous strain broadening due to imperfect microstructural self-accommodation of the martensitic grains. No strain broadening occurs when the martensitic phase is not fully interconnected but forms isolated islands inside an austenite matrix. It is concluded that large stress fields result from the coalescence of martensitic regions in the sample. The calibration of the excess entropy from the measurements of the specific heat confirms the Landau potential of Salje *et al* (2007 *Appl. Phys. Lett.* **90** 221903). Imperfect self-accommodation does not contribute to a measurable increase of the entropy of the sample.

(Some figures in this article are in colour only in the electronic version)

1. Introduction

Most martensitic phase transitions in metals and alloys are strongly discontinuous, which limits the determination of order parameters besides its value zero in the austenite phase and a very narrow interval near unity in the martensitic phase [1]. Intermediate values have no thermodynamic stability while they may still relate to unstable states and they may also be useful for any theoretical description of the transition behavior based on analytical theories [2–8]. Recently the martensitic phase transition in Ni–Al was investigated leading to the first determination of the Landau potential of these materials [9]. It is the purpose of this paper to describe the experimental details of that investigation and to discuss the first observation of residual stresses in the martensitic phase.

Ni_xAl_{100-x} undergoes a martensitic phase transition in the Ni rich composite with excess Ni randomly replacing Al, in the range of $60 < x < 69$. The austenite phase, sometimes referred to as the β_2 phase, has cubic B2 or CsCl type structure at high temperature while the structure of the martensitic phase depends on its chemical composition. For $x > 63$ the structure is $L1_0$ (face centered tetragonal) or 3M with homogeneous $\{110\}\langle 1\bar{1}0\rangle$ shear strain; for $x < 63$ the structure is 7R or 14M with a periodic alternating shuffle of the (110) B2 planes superimposed on the homogeneous strain [10–18].

The phase transition in Ni–Al was extensively studied by various techniques [19–26]. Pre-transformation phenomena and only limited phonon softening above the phase transition were found [19, 20]. Krumhansl *et al* [27] had suggested a generic first order Landau mode free energy to describe these features for transitions with little phonon softening and first order character. In this approach a leading order parameter related to the shuffle or the uniform deformation was invoked. Salje *et al* [9] followed a different approach where a thermodynamic order parameter Q is considered which scales the excess entropy of the transformation (within the framework of Landau theory including low temperature quantum saturation). This order parameter contains, via the appropriate coupling mechanisms, already all relevant physical parameters such as shuffle amplitudes, strains and any other

source of excess entropy. The second step was then to investigate the scaling of the structural strain e with respect to Q. It was found that, within experimental resolution, this scaling is linear so that one may either consider the spontaneous deformation as 'primary' order parameter or, more correctly, to state that the Q has the same scaling as e while other physical excess quantities may still contribute to the transition mechanism (but do not change the overall thermodynamic characteristics of the phase transformation).

The classic Landau potentials for first order phase transition in displacive limit for the relevant symmetry constraints is a 2-4-6 model

$$G(Q) = \tfrac{1}{2}A(T - T_c)Q^2 + \tfrac{1}{4}BQ^4 + \tfrac{1}{6}CQ^6. \quad (1)$$

Although this model can predict the transition behavior at high temperature very well, it is known that this model cannot simply be extrapolated to low temperatures. The underlying difficulty relates to the third law of thermodynamics, which implies that the absolute zero temperature cannot be attained. A direct consequence of this is that $\mathrm{d}Q/\mathrm{d}T \to 0$ as $T \to 0$. The saturation behavior is driven by thermodynamic effects, and not because the order parameter has reached some maximum value, which can never be exceeded.

It is shown that the key feature of the classical Landau potential, that the excess entropy is proportional to Q^2, follows from more general physical models provided that certain approximations are made. These approximations are valid for large values of temperature, and are equivalent to the approximations made when deriving classical physics from the more general quantum mechanical models. A detailed theory of the low temperature saturation was first developed in [28]; further applications for phase diagrams and the application of external fields such as stress field were given in [29, 30].

In the displacive limit, the quantum version of Landau theory of first order phase transitions is expressed by a macroscopic Gibbs free energy [28, 31]:

$$G(Q) = \tfrac{1}{2}A\Theta_s(\coth(\Theta_s/T) - \coth(\Theta_s/T_c))Q^2 + \tfrac{1}{4}BQ^4 + \tfrac{1}{6}CQ^6, \quad (2)$$

where Θ_s is the quantum mechanical saturation temperature which characterizes the effect of zero point vibrations as opposed to thermally activated phonons. T_c is the Curie temperature and A, B, and C are energy scaling parameters related to local potentials [28]. Here the expression is limited to sixth order potentials in order to keep the number of free parameters small; higher order terms were discussed in [3]. The transition is characterized by two temperatures, Θ_s and T_c, therefore. Traditionally studies of phase transitions have focused on T_c while determinations of Θ_s yield useful insights into the behavior of phase transitions, namely the identification of the relevant soft mode branches. Θ_s was found not greatly altered by chemical doping or application of external fields [32].

The driving order parameter Q in the β_2 phase of Ni–Al is coupled bi-linearly with the spontaneous strain. A test for the validity of this approach follows from the scaling of the excess entropy which is related to the order parameter via $S(Q) = \mathrm{d}G(Q)/\mathrm{d}T$. At $T \gg \Theta_s$ this leads to $S = \frac{1}{2}AQ^2$. As the spontaneous strain scales linearly with the order parameter we expect the entropy to scale as $S = S(e^2)$. We will argue that this prediction is confirmed experimentally (see [33] for the similar case of $SrTiO_3$).

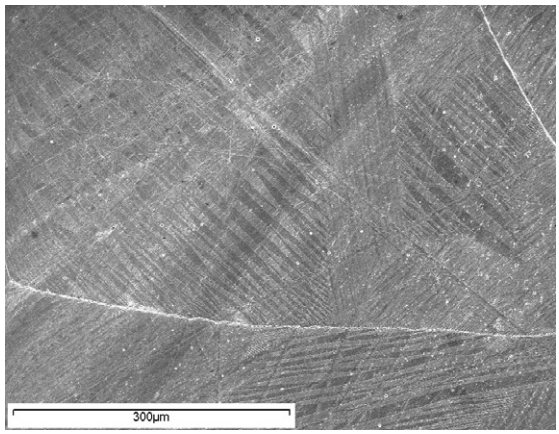

Figure 1. Room temperature SEM image of Ni–Al (I) showing martensitic needle domains and their branching. The grain diameters are around 1 mm.

2. Experiments and results

2.1. Sample preparation

The Ni–Al samples were prepared by melting 99.99% pure elements in an arc furnace. The samples were then homogenized at 1473 K for 5 h in sealed quartz tube and then quenched into iced water. The phase composition and microstructure were evaluated by SEM. Samples with two different compositions were obtained: $Ni_{63.5}Al_{36.5}$ and $Ni_{62}Al_{38}$. The characteristic grain diameter was 1 mm.

For $Ni_{63.5}Al_{36.5}$, two samples with two different quench rates showed different transition temperatures: Ni–Al (I) at 460 K and Ni–Al (II) at 240 K, which may be due to the different order or vacancies-defect configuration (internal stress) generated by the various quenching processes. Their transition temperatures were determined by differential scanning calorimetry (DSC) measurements and by x-ray rocking curve measurements. From the SEM image of Ni–Al (I) shown in figure 1, needle domains of martensite can be seen in the grains. The $Ni_{62}Al_{38}$ shows no phase transition above room temperature. The sample size of Ni–Al (II) for x-ray measurements is $5 \times 5 \times 2$ mm^3. Small pieces of Ni–Al (I) and $Ni_{62}Al_{38}$ were cut for DSC experiments.

2.2. Differential scanning calorimetry experiments

The DSC experiments were performed on a Perkin-Elmer Diamond DSC calorimeter in the conventional scanning mode with a heating/cooling rate of 20 K min^{-1}. The heat flow and temperature was calibrated by standard materials (In, Zn). Apart from the temperature region of the phase transition, the differential heat supplied by a DSC instrument to a sample is proportional to the specific heat capacity at constant pressure of the latter. The specific heat was calculated by comparing

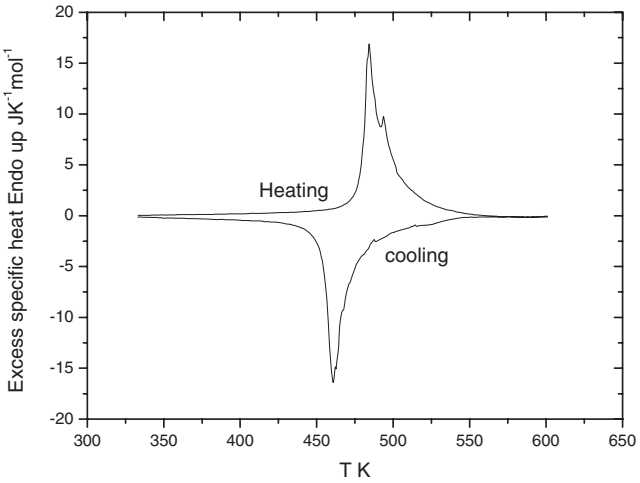

Figure 2. Temperature dependence of the excess specific heat of Ni–Al (I).

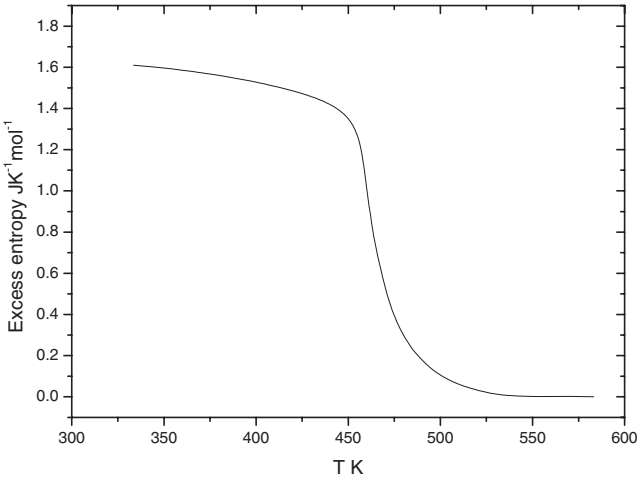

Figure 3. Temperature dependence of the excess entropy of Ni–Al (I).

the deflection of the sample and that of a sapphire standard from the baseline behavior of the empty pan [34]. An austenitic $Ni_{62}Al_{38}$ sample was equally measured, its specific heat served then as baseline for the Ni–Al (I). Subtracting the baseline, the excess specific heat ΔC_p (contribution of latent heat was also included) is then exclusively due to the martensitic phase transition of Ni–Al (I) (figure 2). Endo- and exothermic peak around 470 K upon heating and cooling was observed respectively, with a hysteresis of 23 K. Integrating $-\Delta C_p/T$ in the cooling process leads to the temperature dependence of the excess entropy as shown in figure 3. The excess entropy increases with decreasing temperature; at temperatures above 470 K a long tail exists which is not sensitive to the details of the choice of baseline. The tail may relate to small variation of composition although it may be tempting to relate them to precursor tweed and other dynamic precursor effects. Pre-transformation effects were already observed in Ni–Al as phonon softening at temperatures 100 K above the transition point for $Ni_{63}Al_{37}$ and for $Ni_{62.5}Al_{37.5,}$ and a tweed structure at room temperature in $Ni_{63}Al_{37}$ and $Ni_{62.5}Al_{37.5}$ [19, 26, 35]. Previous thermal expansion measurements on a $Ni_{62.5}Al_{37.5}$ single crystal showed pre-transformation effects starting 115 K above the transition point [22]. The pre-martensitic temperature interval of the tail in the excess entropy is smaller than those reported in [22], which may be due to the different composition of samples.

To check the scaling of S with respect to e^2, the lattice parameter data of the Ni–Al sample with similar transition temperature from [25] were compared with our excess entropy data in figure 4. In order to compare these data we rescaled the transition temperature in [25] to coincide with ours and constrained the origin of e and S by the condition that $e = 0$ at $S = 0$. The most uncertain variable is Θ_s. These uncertainties are demonstrated in figure 4 where three fits with three different values of Θ_s are shown to reproduce the experimental values equally well using our experimental data. The value of Θ_s remains poorly constraints within a large interval between 100 and 300 K. Independently, the value of

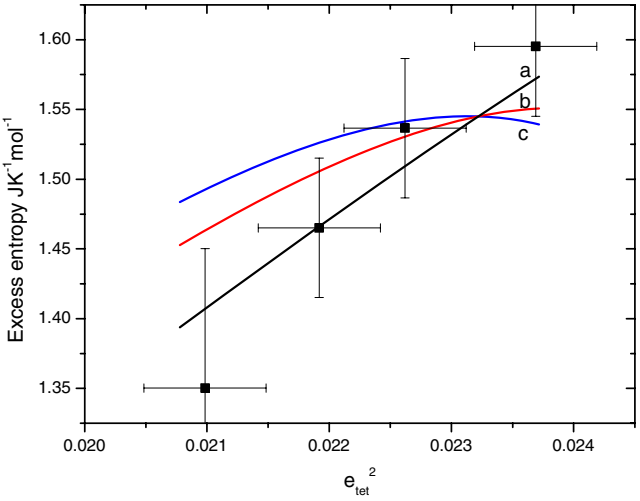

Figure 4. Excess entropy versus e^2. The fit lines shows the relation $S(Q) = \mathrm{d}G(Q)/\mathrm{d}T$ between them with different saturation temperatures: a: $\Theta_s = 100$ K; b: $\Theta_s = 250$ K; c: $\Theta_s = 300$ K.

Θ_s can be estimated via its empirical relationship with the thermodynamic Einstein temperature Θ_E [36]:

$$\Theta_s = \tfrac{1}{2}\Theta_{E.}$$

In case of Ni–Al the Einstein temperature is 500 K so that we set Θ_s at 250 K as the initial value [23]. This value is similar to the value obtained from fitting of spontaneous strain data of Ni–Al (II) as discussed later. As the Θ_s does not change too much with chemical doping as mentioned above, the setting of Θ_s at 250 K appears to be reasonable. The fitting of the excess entropy with equations (2) with Θ_s fixed at 250 K is shown in figure 5. Figure 6 shows the thermodynamic potentials (as molar excess free energy) versus order parameter at different temperatures. 512 K is the highest temperature where a local free energy minimum for the martensitic phase still exists, which roughly agrees with the temperature interval of the tail of the excess entropy in figure 3.

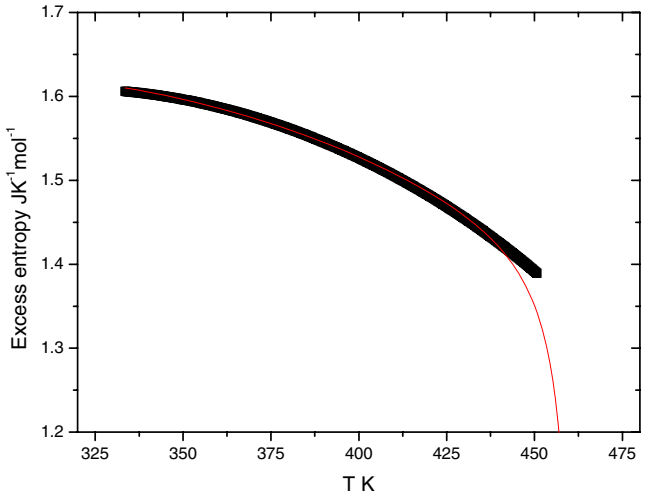

Figure 5. Temperature dependence of excess entropy of Ni–Al (I) and the fit line with $G(Q) = \frac{1}{2}A\Theta_s(\coth(\Theta_s/T) - \coth(\Theta_s/T_c))$ $Q^2 + \frac{1}{4}BQ^4 + \frac{1}{6}CQ^6$ with $A = 5.6$ J K^{-1} mol^{-1}, $B = -5038$ J mol^{-1}, $C = 7491$ J mol^{-1}, $T_c = 338$ K, and $\Theta_s = 250$ K.

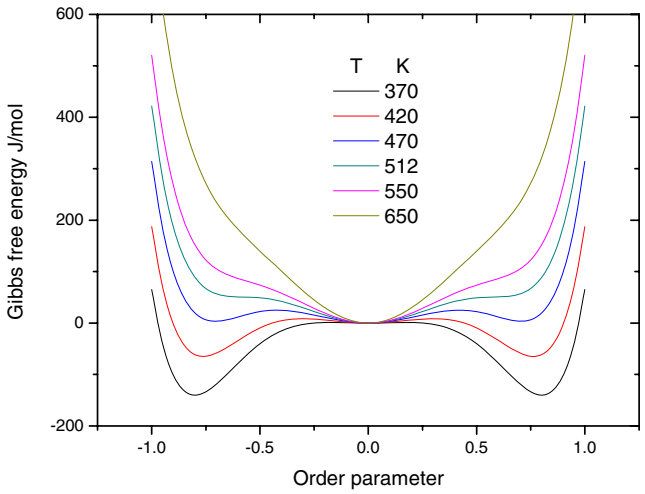

Figure 6. Gibbs free energy at different temperatures for Ni–Al (I).

2.3. X-ray diffraction experiments

X-ray diffraction (XRD) experiments were conducted using monochromatic Cu Kβ radiation and a position sensitive detector with an angular range 2θ of 120°. The distance between two channels is equivalent to $\Delta(2\theta) = 0.018°$, the instrumental linewidth of the diffraction signal is $\delta(2\theta) = 0.08°$. In this experimental arrangement, the sample holder was tilted around an axis perpendicular to the x-ray beam, making it possible to record intensity-2θ spectra at different rocking angle ω [37]. The angular resolution of the rocking movement is 0.001°. For regular measurements, the sample holder continually rocks in an angular range where the x-ray peaks locate.

Figure 7 shows the 211 peak of austenite (B2) and 311 peak of martensite ($L1_0$) of Ni–Al (II) as a function of temperature under cooling. Crystallographically, the peaks

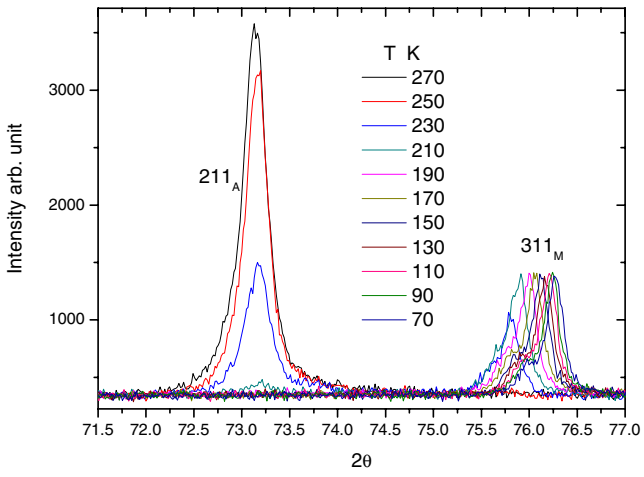

Figure 7. X-ray spectrum of Ni–Al (II) on cooling.

observed in the austenite and martensite originate from the equivalent lattice planes in the two phases. We now analyze the diffraction signal in terms of the spontaneous strain of the martensitic transformation and its heterogeneous strain broadening. For transitions from cubic to face centered tetragonal, the symmetry adapted spontaneous strains are given by

$$e_{\text{vol}} = (e1 + e2 + e3)/\sqrt{3}$$

$$e_{\text{tetr}} = (2e3 - e1 - e2)/\sqrt{6}$$

where

$$e1 = e2 = \frac{\frac{a}{\sqrt{2}} - a_0}{a_0}$$

$$e3 = \frac{c - a_0}{a_0}$$

a and c are lattice parameters of the martensitic phase while a_0 is the extrapolation of the lattice parameter of the austenite phase into the temperature region of the martensitic phase. The tetragonal strain is a tetragonal lattice distortion without change of the cell volume, which is related to the $\{110\}\langle 1\bar{1}0\rangle$ shear strain in Ni–Al. No volume strain is considered in our analysis. In order to calculate the spontaneous strain, the lattice parameters of austenite are extrapolated into the temperature regime of martensite to reduce the part of thermal expansion which is not related to the phase transition. The spontaneous strain increases with decreasing temperature below the transition temperature with a discontinuity at the transition temperature with zero for the austenite phase (figure 8). The calibration of the order parameter was then done in the following way. By definition the order parameter has the value 1 at absolute zero temperature when quantum saturation is ignored. We maintain this traditional calibration by switching mathematically the quantum saturation off (i.e. setting Θ_s to zero). The Landau coefficients are then calculated to obtain $Q = 1$ at $T = 0$ K. We then change Θ_s back to the experimental value of 257 K. This means that the order parameter Q at $T = 0$ K is reduced

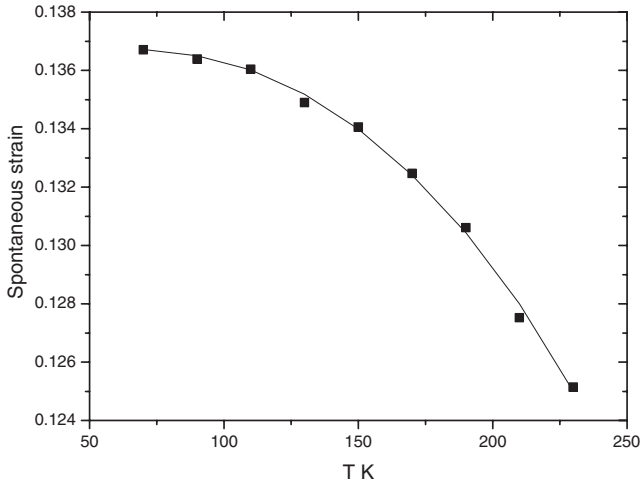

Figure 8. Temperature evolution of the spontaneous strain in Ni–Al (II); the Landau potentials parameter of the fit line are the same as shown in figure 9.

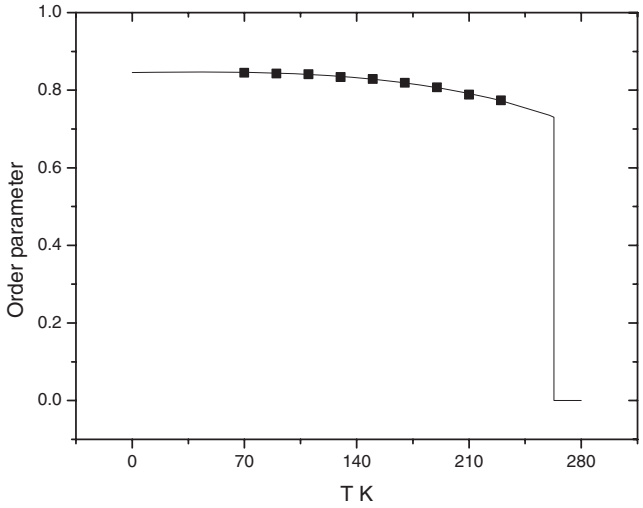

Figure 9. Temperature dependence of order parameter and fit line with $G(Q) = \frac{1}{2}A\Theta_s(\coth\Theta_s/T) - (\coth(\Theta_s/T_c))Q^2 + \frac{1}{4}BQ^4 + \frac{1}{6}CQ^6$ with $A = 5.6$ J K^{-1} mol^{-1}, $B = -3493$ J mol^{-1}, $C = 4901$ J mol^{-1}, $T_c = 86$ K, and $\Theta_s = 257$ K.

to 0.846 which is in agreement with theory [28]. The resulting Landau potentials are shown in figure 9.

For a martensitic phase transition, the microstructure of the martensite is thought to be determined by self accommodation between different variants to minimize the elastic strain energy. The resulting heterogeneous strain is then expected to be small, i.e. below experimental resolution. This is not the case in our samples. Significant strain broadening is seen in the rocking curves in figure 10. In order to quantify the broadening the contours in figure 10 were re-measured at different rocking angle ω with a step-width of 0.1°. The two maxima (211 peak of austenite and 311 peak of martensite) were identified to originate from two grains with a 0.6° grain boundary (each grain forms an individual pole in this experimental arrangement). The contour lines of 211 of austenite for the grain at lower rocking angle shows 45° tilting, indicating some texture caused by aggregating of defects or small variation of composition which leads to a small gradient of the lattice parameter. The martensitic grains show roughly circular contour lines with no significant elongation along the Bragg angle which is indicative for stress free particles. The intensities of the rocking curves were then integrated for rocking angles perpendicular to the Bragg angle so that the resulting peak is equivalent of a powder diffraction peak. This peak was fitted with Lorentz function to obtain the peak intensity and the full width at half maximum (FWHM). Figure 11 shows the FWHM and the relative peak intensities of the martensite 311 and austenite 211 peaks across the phase transition. It can be seen that the FWHM of martensitic 311 increases with decreasing temperature in the phase transition region to a maximum at a temperature where the transition is completed. This trend was reversible under heating. The FWHM of austenite 211 followed a similar increase with decreasing temperature. Without detailed knowledge of the precise microstructure our observations can be understood as follows. Under cooling through the phase transition temperature the martensitic phase nucleates. The nuclei show virtually no strain broadening so that the transformation strain appears to be fully compensated by the appropriate microstructure within each martensitic region. We find increasing strain broadening when the transformation process proceeds. It can be assumed that increasingly larger martensitic regions interact with each other which may lead to highly strained interfaces between different martensitic variants. A similar observation was reported by Boullay *et al* [38] who saw tapping, bending and tip splitting of smaller microtwin variants in a region of approximately 5–10 nm width around the macrotwin interfaces and a variety of structural defects further away from the interfaces, which also shows the influence of residual stress at the interfaces. The heterogeneous strain as observed in our rocking experiment decreases slightly with decreasing temperature showing that a somewhat higher degree of strain accommodation is achieved at lower temperatures. Note that at these temperatures the order parameter is not fully saturated and that small increases of lattice deformations still occur when cooling the sample (figure 8). As the effect is reversible it is unlikely that the additional strain accommodation is an entirely kinetic effect. Nevertheless, our observation clearly indicates that some strain reduction by changes of microstructure is still observed at temperatures as low as 150 K indicating a low activation energy of interfacial movements. Low activation energies of twin boundary movements were also found in ferroelastic materials with recorded movements as low as 20 K [39, 40].

3. Conclusion

DSC and x-ray diffraction experiments were undertaken on two $Ni_{63.5}Al_{36.5}$ samples with different transition temperatures. The excess entropy and the spontaneous strain of the phase transition were determined from the DSC data and x-ray

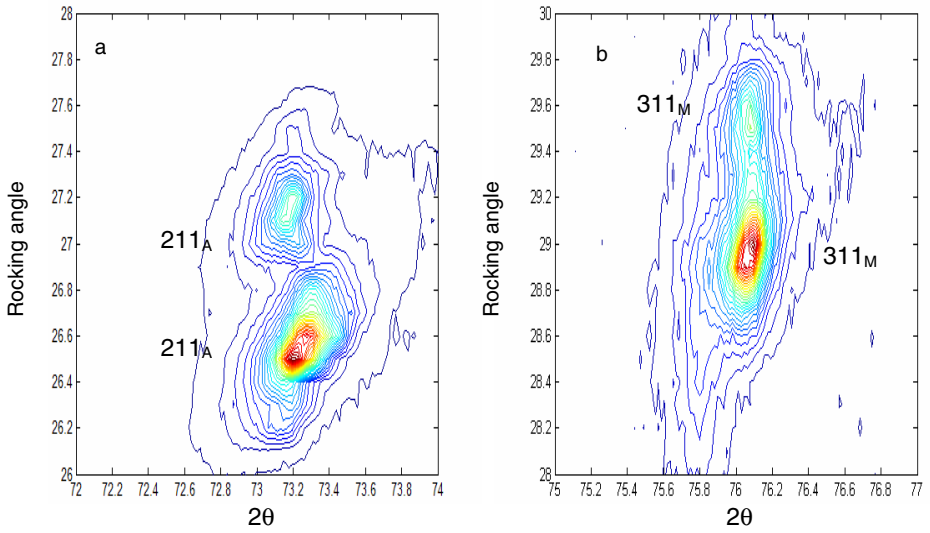

Figure 10. (a) The contour lines of the intensity of the 211 peak of austenite at 265 K; (b) the contour lines of the intensity of the 311 peak of martensite at 180 K.

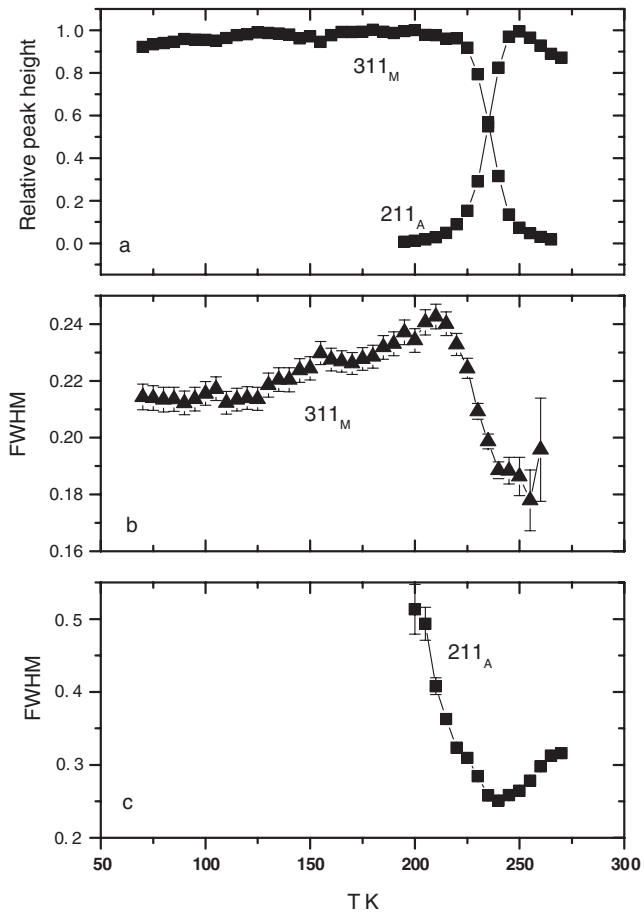

Figure 11. (a) The relative peak height of 311 of martensite and 211 of austenite on cooling; (b) FWHW of 311 of martensite on cooling; (c) FWHW of 211 of austenite on cooling.

data, respectively. Landau potentials were determined for the phase transition by fitting the data with Landau theory. Heterogeneous strain broadening of diffraction profiles was observed and discussed in term of imperfect microstructural self accommodation of the martensitic grains once these grains coalesce at sufficiently low temperatures.

Acknowledgment

EKHS, HZ and BB acknowledge the support from Marie-Curie RTN Multimat (contract no. MRTN-CT-2004-505226).

References

[1] Otsuka K and Wayman C M 1998 *Shape Memory Materials* (Cambridge: Cambridge University Press)
[2] Falk F 1989 *Int. J. Eng. Sci.* **27** 277
[3] Barsch G R and Krumhansl J A 1984 *Phys. Rev. Lett.* **53** 1069
[4] Gooding R G and Krumhansl J A 1988 *Phys. Rev.* B **38** 1695
[5] Kartha S, Kastan T, Krumhansl J A and Sethna J P 1991 *Phys. Rev. Lett.* **67** 3630
[6] Ahluwalia R, Lookman T, Saxena A and Albers R C 2004 *Acta Mater.* **52** 209
[7] Jin Y M, Artemev A and Khachaturyan A G 2001 *Acta Mater.* **49** 2309
See also Khachaturyan A G 1983 *Theory of Structural Transformations in Solids* (New York: Wiley) as earlier review
[8] Wang X, Mainville J, Ludwig K, Flament X, Finel A and Caudron R 2005 *Phys. Rev.* B **72** 024215
[9] Salje E K H, Zhang H, Schryvers D and Bartova B 2007 *Appl. Phys. Lett.* **90** 221903
[10] Enami K, Nenno S and Shimizu K 1973 *Trans. JIM* **14** 161
[11] Chakravorty S and Wayman C M 1976 *Metall. Trans.* A **7** 569
[12] Au Y K and Wayman C M 1972 *Scr. Metall.* **6** 1209
[13] Smialek J L and Hehemann R F 1973 *Metall. Trans.* **4** 1571
[14] Reynaud F 1977 *Scr. Metall.* **11** 765
[15] Martynov V V, Enami K, Khandros L G, Tkachenko A V and Nenno S 1983 *Scr. Metall.* **17** 1167
[16] Otsuka K, Ohba T, Tokonami M and Wayman C M 1993 *Scr. Metall. Mater.* **19** 1359
[17] Martynov V Y, Enami K, Khandros L G, Nenno S and Tkachenko A V 1983 *Phys. Met. Metallogr. (USSR)* **55** 136

[18] Noda Y, Shapiro S M, Shirane G, Yamada Y and Tanner L E 1990 *Phys. Rev.* B **42** 10397
[19] Shapiro S M, Yang B X, Noda Y, Tanner L E and Schryvers D 1991 *Phys. Rev.* B **44** 9301
[20] Shapiro S M, Larese J Z, Noda Y, Moss S C and Tanner L E 1986 *Phys. Rev. Lett.* **57** 3199
[21] Davenport T, Zhou L and Trivisonno J 1999 *Phys. Rev.* B **59** 3421
[22] Liu M, Finlayson T R and Smith T F 1992 *Mater. Sci. Eng.* A **157** 225
[23] Rubini S, Dinmitropoulos C, Aldrovandi S, Borsa F, Torgeson D R and Ziolo J 1992 *Phys. Rev.* B **46** 10563
[24] Kelley D and Louca D 2005 *Scr. Mater.* **53** 475
[25] Potapov P L, Poliakova N A and Udovenko V A 1996 *Scr. Mater.* **35** 423
[26] Schryvers D and Tanner L E 1990 *Ultramicroscopy* **32** 241
[27] Krumhansl J A and Gooding R J 1989 *Phys. Rev.* B **39** 3047
[28] Salje E K H, Wruck B and Thomas H 1991 *Z. Phys.* B **82** 399
[29] Pérez-Mato J M and Salje E K H 2001 *Phil. Mag. Lett.* **81** 885
[30] Pérez-Mato J M and Salje E K H 2000 *J. Phys.: Condens. Matter* **12** L29
[31] Salje E K H 1993 *Phase Transitions in Ferroelastic and Co-elastic Crystals* (Cambridge: Cambridge University Press)
[32] Hoyward S A and Salje E K H 1998 *J. Phys.: Condens. Matter* **10** 1421
[33] Salje E K H, Gallardo M C, Jiménez J, Romero F J and del Cerro J 1998 *J. Phys.: Condens. Matter* **10** 5535
[34] Gilmour I W and Hay J N 1977 *Polymer* **18** 281
[35] Tanner L E, Pelton A R, VanTendeloo G, Schryvers D and Wall M E 1990 *Scr. Mater.* **24** 1731
[36] Salje E and Wruck B 1991 *Ferroelectrics* **124** 185
[37] Chrosch J and Salje E K H 1999 *J. Appl. Phys.* **85** 722
[38] Boullay Ph, Schryvers D and Ball J M 2003 *Acta Mater.* **51** 1421
[39] Kityk A V, Schranz W, Sondergeld P, Havlik D, Salje E K H and Scott J F 2000 *Phys. Rev.* B **61** 946
[40] Harrison R J, Redfern S A T and Salje E H K 2004 *Phys. Rev.* B **69** 144101